4662–4676 *Nucleic Acids Research, 2018, Vol. 46, No. 9* *Published online 10 April 2018*
doi: 10.1093/nar/gky243

A natural non-Watson–Crick base pair in human mitochondrial tRNA^{Thr} causes structural and functional susceptibility to local mutations

Yong Wang[1,2], Qi-Yu Zeng[1], Wen-Qiang Zheng[2], Quan-Quan Ji[1], Xiao-Long Zhou[1,*] and En-Duo Wang[1,2,*]

[1]State Key Laboratory of Molecular Biology, CAS Center for Excellence in Molecular Cell Science, Shanghai Institute of Biochemistry and Cell Biology, Chinese Academy of Sciences; University of Chinese Academy of Sciences, 320 Yueyang Road, Shanghai 200031, P.R. China and [2]School of Life Science and Technology, ShanghaiTech University, 100 Haike Road, Shanghai 201210, P.R. China

Received January 17, 2018; Revised March 19, 2018; Editorial Decision March 20, 2018; Accepted March 26, 2018

ABSTRACT

Six pathogenic mutations have been reported in human mitochondrial tRNA^{Thr} (hmtRNA^{Thr}); however, the pathogenic molecular mechanism remains unclear. Previously, we established an activity assay system for human mitochondrial threonyl-tRNA synthetase (hmThrRS). In the present study, we surveyed the structural and enzymatic effects of pathogenic mutations in hmtRNA^{Thr} and then focused on m.15915 G > A (G30A) and m.15923A > G (A38G). The harmful evolutionary gain of non-Watson–Crick base pair A29/C41 caused hmtRNA^{Thr} to be highly susceptible to mutations disrupting the G30–C40 base pair in various ways; for example, structural integrity maintenance, modification and aminoacylation of tRNA^{Thr}, and editing mischarged tRNA^{Thr}. A similar phenomenon was observed for hmtRNA^{Trp} with an A29/C41 non-Watson–Crick base pair, but not in bovine mtRNA^{Thr} with a natural G29–C41 base pair. The A38G mutation caused a severe reduction in Thr-acceptance and editing of hmThrRS. Importantly, A38 is a nucleotide determinant for the t^{6}A modification at A37, which is essential for the coding properties of hmtRNA^{Thr}. In summary, our results revealed the crucial role of the G30–C40 base pair in maintaining the proper structure and function of hmtRNA^{Thr} because of A29/C41 non-Watson–Crick base pair and explained the molecular outcome of pathogenic G30A and A38G mutations.

INTRODUCTION

Mitochondria are present in most eukaryotic cells and generate the majority of cellular energy via oxidative phosphorylation (1). Mitochondria have their own genome and protein synthesis system. The human mitochondrial genome encodes 13 essential subunits of respiratory chain complexes, two rRNAs, and 22 mitochondrial tRNAs (hmtRNAs) (2). In the mitochondrial translation system, the RNA components are supplied by the mitochondria, whereas the protein components, such as ribosomal proteins, aminoacyl-tRNA synthetases (aaRSs), and various factors, are encoded in nucleus and transported into the mitochondria from the cytoplasm (3).

In human mitochondria, all amino acids occupy only one corresponding hmtRNA, except for two copies for hmtRNA^{Ser} and hmtRNA^{Leu}. To date, more than 250 pathogenic mutations associated with mitochondrial diseases have been reported in hmtRNAs genes (http://www.mitomap.org/MITOMAP) (4), indicating the essential role of hmtRNAs in mitochondrial functions. These mutations affect the stability and functions of tRNAs (5,6). For example, the mitochondrial myopathy, encephalopathy, lactic acidosis, and stroke-like episodes syndrome (MELAS)-associated mutations in hmtRNA^{Leu} (UUR) result in marked reduction in aminoacylation and a fragile structure (7). The U48C mutation causes T-stem slip in hmtRNA^{Leu} (CUN) (8). The A8344G mutation in hmtRNA^{Lys} causes the abolition of the m^{5}s^{2}U modification, resulting in severe translation failure in myoclonic epilepsy with ragged red fibers (MERRF) (9,10). The G52A and A57G mutations in hmtRNA^{Leu} (CUN) and hmtRNA^{Leu} (UUR) lead to lower stability and decreased tRNA charging capacity (11). These observations imply that functional defects of tRNAs play a key role in mitochondrial translation and molecular pathogenesis.

*To whom correspondence should be addressed. Tel: +86 21 5492 1241; Fax: + 86 21 5492 1011; Email: edwang@sibcb.ac.cn
Correspondence may also be addressed to Xiao-Long Zhou. Tel: +86 21 5492 1242; Fax: +86 21 5492 1011; Email: xlzhou@sibcb.ac.cn

The pivotal role of tRNA is to generate aminoacyl-tRNA, catalyzed by aaRS, as the first step of protein biosynthesis. The aminoacylation reaction requires a high level of accuracy and provides a critical checkpoint for translational quality control (12). Some aaRSs have evolved editing functions to ensure removal of incorrect aa-AMPs (pre-transfer editing) or mis-charged tRNAs (post-transfer editing) (13,14). A slight decrease in cytoplasmic aminoacylation accuracy could cause an intracellular accumulation of mis-folded proteins and upregulation of protein chaperones in neurons, causing severe mammalian neurodegeneration (15). Similarly, impaired mitochondrial aminoacylation accuracy leads to embryonic lethality (16).

We have cloned *TARS2*, encoding the human mitochondrial threonyl-tRNA synthetase (hmThrRS) precursor, and purified the mature form of hmThrRS. hmThrRS is active in hmtRNA^{Thr} aminoacylation and utilizes tRNA-dependent pre-transfer editing and post-transfer editing to maintain translational quality control. Establishing such an aminoacylation and editing determination system enables us to further study the molecular basis of the potential pathogenic mechanism for hmtRNA^{Thr} in amino acid charging. So far, six mutations in the hmtRNA^{Thr} gene have been reported as pathogenic. A patient carrying the m.15915 G > A (G30A) mutation in hmtRNA^{Thr} gene displayed hearing loss, muscle weakness, mental retardation, and seizures (17). The m.15923A > G (A38G) mutation caused lethal infantile mitochondrial myopathy (LIMM) and the patients showed hypoglycemia, lactic acidosis, and sudden multisystem failure (18). The m.15924A > G (A39G) mutation led to lethal respiratory chain defects and was fatal in infancy (19). A patient carrying the Δ15940U (ΔU60) mutation showed Leber's hereditary optic neuropathy (LHON) (20). The m.15950 G > A (G70A) mutation was associated with Parkinson's disease, which could contribute to dopaminergic nerve cell death (21). A patient carrying the m.15951A > G (A71G) mutation exhibited loss of vision (22). However, their molecular mechanisms need to be explored.

tRNAs acquire a large variety of modifications during the maturation process. Among these, the N^6-threonylcarbamoyladenosine (t^6A) modification, which is often located at position 37, aroused our interest. The t^6A modification is found in almost all tRNAs reading ANN codons (N being one of the four nucleotides A, C, G and U) of all three kingdoms: bacteria, eukaryotes, and archaea, and also in mitochondria and chloroplasts (23). The t^6A modification facilitates codon-anticodon interaction and promotes translational fidelity (24,25). Deficiency of the t^6A modification leads to an obvious increase in frameshifting events in cells (26). Although the enzymes responsible for the t^6A modification of mammalian mitochondrial tRNAs have not been identified, the *in vitro* t^6A biosynthesis reaction using *Saccharomyces cerevisiae* Sua5 and Qri7 have been established (27). Sua5 catalyzes threonine, bicarbonate, and ATP to generate the intermediate threonylcarbamoyl-AMP (TCA) (28). TCA is then released from Sua5 and is bound by Qri7 to participate in the t^6A modification (27). According to previous reports, one of the pathogenic mutations of hmtRNA^{Thr}, A38G, is next to t^6A37 of tRNAs. The t^6A modification occurs at A37 in bovine mitochondrial tRNA^{Thr} (bmtRNA^{Thr}), suggesting that hmtRNA^{Thr} likely has a t^6A modification. We are interested in whether hmtRNA^{Thr} could be t^6A-modified *in vitro* and, if so, what are the effects of these pathogenic mutations on the modification of t^6A37?

In the present study, based on initial structural and functional screen of all pathogenic mutations, we focused on the G30A and A38G mutations, which are located in the anticodon stem and loop of hmtRNA^{Thr} (Figure 1A). We revealed the intrinsic susceptibility of the anticodon stem in terms of structural integrity, aminoacylation, editing, and tRNA modification, which was caused by an evolutionary non-Watson–Crick A29/C41 base pair in hmtRNA^{Thr}. Furthermore, A38 contributes significantly to aminoacylation and editing, and is a determinant for the t^6A modification. Our results provide clues to the potential molecular mechanisms of pathological hmtRNA mutations.

MATERIALS AND METHODS

Materials

L-Thr, L-Ser, dithiothreitol, nucleoside triphosphates (NTPs), guanosine monophosphate (GMP), tetrasodium pyrophosphate, Tris-base, $MgCl_2$, NaCl and inorganic pyrophosphate were purchased from Sigma (St Louis, MO, USA). [^{14}C]Thr was obtained from Biotrend Chemicals (Destin, FL, USA). [α-^{32}P]ATP and [γ-^{32}P]ATP were obtained from Perkin Elmer Inc. (Waltham, MA, USA). T4 DNA ligase, T4 PNK (polynucleotide kinase), RNase T1, RNase S1, and restriction endonucleases were obtained from Thermo Scientific (Pittsburgh, PA, USA). Phusion high-fidelity DNA polymerase was purchased from New England Biolabs (Ipswich, MA, USA). Ni^{2+}-NTA (nitrilotriacetic acid) Superflow was purchased from Qiagen Inc. (Germany). Pyrophosphatase (PPiase) was obtained from Roche Applied Science (China). The dNTP mixture was purchased from Takara (Japan). Oligonucleotide primers were synthesized by Biosune (China). *Escherichia coli* Rosetta (DE3) cells were purchased from Stratagene (Santa Clara, CA, USA).

tRNA gene cloning and transcription

The mitochondrial genomes of humans and cows contain only one gene encoding mtRNA^{Thr} with a UGU anticodon. Construct pTrc99b-T7-hmtRNA^{Thr} was obtained as described previously (29). The DNA sequence of the T7 promoter and the bovine mitochondrial tRNA^{Thr} (bmtRNA^{Thr}) gene were obtained by ligating six chemically synthesized DNA fragments together, and then ligating the product into plasmid pTrc99b (pre-cleaved with EcoRI/BamHI) to construct pTrc99b-T7-bmtRNA^{Thr}. The DNA fragment (Transzyme^{Trp}) containing the DNA sequence of the T7 promoter, hammerhead ribozyme, and the hmtRNA^{Trp} gene was cloned from eight chemically synthesized DNA fragments using the same protocol as that for bmtRNA^{Thr} (30). Gene mutagenesis was performed according to the protocol provided with the KOD-plus mutagenesis kit. Transcripts were obtained using the T7 RNA polymerase run-off procedure, as described previously (31). The

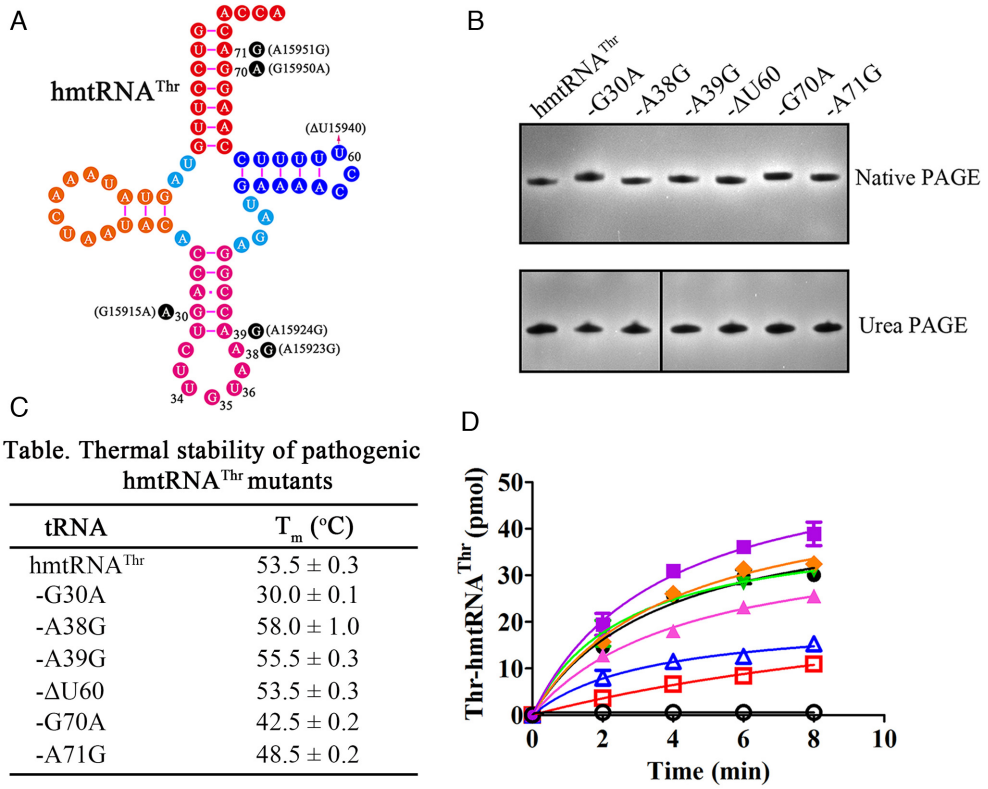

Table. Thermal stability of pathogenic hmtRNA^{Thr} mutants

tRNA	T_m (°C)
hmtRNA^{Thr}	53.5 ± 0.3
-G30A	30.0 ± 0.1
-A38G	58.0 ± 1.0
-A39G	55.5 ± 0.3
-ΔU60	53.5 ± 0.3
-G70A	42.5 ± 0.2
-A71G	48.5 ± 0.2

Figure 1. Cloverleaf structure and stability of hmtRNA^{Thr} and its mutants. (**A**) Cloverleaf structure of hmtRNA^{Thr} with pathogenic mutations. (**B**) Analysis of the conformations of the pathogenic mutants under native and denaturing conditions. (**C**) T_m values of pathogenic mutants. (**D**) Aminoacylation of pathogenic related mutants. hmtRNA^{Thr} (●), -G30A (□), -A38G (△), -A39G (▽), -U60 (◆), -G70A (▲), -A71G (■) and without enzyme addition as control (○). Error bars indicate the standard deviations.

tRNA concentration was determined by UV absorbance at 260 nm and the extinction coefficient was calculated from the sequence of each tRNA. The hmtRNA^{Thr} transcript has an excellent amino acid accepting capacity (~1400 pmol/A_{260}), suggesting that it is correctly folded without modification.

Gene cloning, mutagenesis, expression, and protein purification

The yeast *Sua5* and *Qri7* coding sequences were amplified from genomic DNA obtained from yeast cells and cloned into vector pET28a(+) with an N-terminal His_6-tag and named pET28a(+)-*Sua5* and pET28a(+)-*Qri7*. pET28a(+)-*Qri7* was used as the template to construct N-terminal truncation mutant pET28a(+)-*Qri7*-ΔN29, which encoded the mature form of *Sc*Qri7. pET28a(+)-*TARS2*-ΔN19 was obtained as detailed previously (29). The *WARS2* coding sequence was amplified from cDNA, obtained by reverse-transcription polymerase chain reaction (RT-PCR) from total RNA obtained from HEK293T cells, and cloned into pET28a(+), with an N-terminal His_6-tag, between EcoRI and XhoI sites. The recombinant plasmid was named pET28a(+)-*WARS2*. pET28a(+)-*WARS2* was used as the template to construct pET28a(+)-*WARS2*-ΔN18 with the sequence encoding the mitochondrial targeting signal deleted (32). The *Sc*Sua5, *Sc*Qri7-ΔN29, hmThrRS-ΔN19, and hmTrpRS-ΔN18 genes were expressed in *E. coli* Rosetta (DE3) cells. Protein overexpression was induced at an A_{600} ≈ 0.6 with 200 μM isopropyl β-D-1-thiogalactopyranoside (IPTG) at 20 °C overnight. Purification of the *Sc*Sua5, *Sc*Qri7-ΔN29, hmThrRS-ΔN19 and hmTrpRS-ΔN18 proteins was performed as described previously (29). The protein concentrations were determined by the A_{280} of the enzyme solution.

Aminoacylation assay

Aminoacylation kinetics were performed at 37°C in a reaction mixture containing 60 mM Tris–HCl (pH 7.5), 10 mM $MgCl_2$, 5 mM dithiothreitol (DTT), 0.1 mg/ml bovine serum albumin (BSA), 2.5 mM ATP, 100 μM [^{14}C]Thr, (0.5–10) μM wild-type hmtRNA^{Thr} or its variants, and 200 nM hmThrRS, as described previously (33). Aminoacylation of hmtRNA^{Trp} with [^{14}C]Trp was carried out at 37°C in a reaction mixture containing 50 mM Tris–HCl (pH 8.0), 10 mM $MgCl_2$, 1 mM KF, 4 mM ATP, 100 μM [^{14}C]Trp, 5 μM hmtRNA^{Trp} or its mutants and 50 nM hmTrpRS.

[^{32}P]-labeling of mtRNA^{Thr} and preparation of Ser-[^{32}P]mtRNA^{Thr}

An editing-defective ThrRS was used to mischarge mtRNA^{Thr}s with Ser to obtain Ser-mtRNA^{Thr} (22). We labeled the mtRNA^{Thr}s and their variants with α-^{32}P-ATP

to obtain ^{32}P labeled tRNAs and aminoacyl-tRNAs, as described previously (29).

tRNA secondary structure probing

tRNA transcripts were labeled with 10 pmol of γ-^{32}P-ATP and T4 PNK enzyme (NEB). Labeled tRNAs were purified on a 12% PAGE gel containing 8 M urea and eluted overnight at 4°C in 600 μl of elution buffer (0.2 M NaAc, pH 5.2). The labeled tRNAs were then precipitated using ethanol, and the pellets were dissolved in 40 μl of 5 mM $MgCl_2$ buffer. Before use, each tRNA transcript was folded by incubation at 80°C for 2 min and then chilled on ice for 5 min.

Structure probing assays were performed as described previously (11,34). In native conditions, labeled tRNAs were digested with RNase S1 at 37°C for 5 min in 5 μl of 10 mM Tris–HCl (pH 7.0), 10 mM $MgCl_2$, 50 mM KCl, and RNase S1 (2.5 or 5 units) (35,36). Under denaturing conditions, the labeled tRNAs were digested with RNase T1 (0.05 units) in 5 μl of 10 mM sodium citrate (pH 5.0), 1 mM EDTA, and 3.5 M urea at 37°C for 5 min. Alkaline ladders were obtained by digestion of the labeled transcript by 5 μl of 80 mM Na_2CO_3/$NaHCO_3$ (pH 9.0) for 5 min at 80°C. All the reactions were stopped by adding 5 μl of stop mixture containing 0.6 M sodium acetate (pH 5.0) and 3 mM EDTA. Cleaved fragments were analyzed on 15% denaturing PAGE containing 8 M urea. Electrophoresis was carried out at 4°C and constant 30 W (∼1500 V) for 4.5 h. Gels were dried for 2 h at 80°C using a Gel Dryer (Bio-Rad), and detected using a phosphorimager (Fujifilm).

AMP formation assay

The AMP formation assay was performed using thin-layer chromatography (TLC) at 37°C in a reaction mixture containing 60 mM Tris–HCl (pH 7.5), 10 mM $MgCl_2$, 5 mM DTT, 0.1 mg/ml BSA, 10 U/ml PPiase (Roche), 40 mM Ser, 3 mM [α-^{32}P]ATP and 2 μM hmThrRS in the presence of hmtRNA^{Thr} or its variants, as detailed previously (29).

Post-transfer editing assay

Post-transfer editing of wild-type pre-formed Ser-[^{32}P]hmtRNA^{Thr} or Ser-[^{32}P]bmtRNA^{Thr} and its variants by hmThrRS was performed as described previously (29).

Biolayer interferometry

The dissociation constant (K_d) was obtained through biolayer interferometry using an Octet RED system (ForteBio). Samples or buffer were dispensed into 96-well plates at 200 μl per well. The operating temperature was maintained at 25°C. Proteins were diluted into kinetic buffer [50 mM potassium phosphate (pH 5.5), 50 mM $MgCl_2$, and 0.002% Tween-20] and immobilized on anti-Ni–NTA sensor tips. The hmtRNA^{Thr} or its variants were diluted with the same buffer into a range of different concentrations. The K_d values were obtained by fitting the processed data with the 1:1 model in the Octet analysis software with $R^2 > 0.99$ and are shown as mean ± error of fit.

In vitro assay for t^{6}A modification of hmtRNA^{Thr}

The reaction was performed at 30°C in a reaction mixture containing 50 mM Tris–HCl (pH 8.0), 200 mM NaCl, 5 mM $MnCl_2$, 1 mM $NaHCO_3$, 2 mM DTT, 2.5 mM ATP, 100 μM [^{14}C]Thr, 5 μM hmtRNA^{Thr} or its variants and 2 μM *Sc*Sua5 and *Sc*Qri7. Samples of the reaction mixture were removed at specific time points, quenched on Whatman filter pads, and equilibrated with 5% trichloroacetic acid. The pads were washed three times for 10 min each with 5% trichloroacetic acid and then with 100% ethanol. The pads were then dried and quantified using a scintillation counter (Beckman Coulter).

RESULTS

Screening of pivotal sites among pathogenic mutations of hmtRNA^{Thr} based on potential structural alterations and aminoacylation defects

To date, six mutations have been reported to be pathogenic in the hmtRNA^{Thr} gene [see Mamit-tRNA database (http://mamit-trna.u-strasbg.fr/Summary.asp)]: G30A, A38G, A39G, G70A, A71G, and U60 deletion (ΔU60) (Figure 1A). The G30A, A38G, and A39G mutations are located in the anticodon stem or loop. The G70A and A71G mutations are in the amino acid-accepting stem. The ΔU60 mutation is in the T loop. However, their effects on the structure and functions of hmtRNA^{Thr} are poorly understood.

To investigate the effect of the above mutations on the structure of hmtRNA^{Thr}, we transcribed hmtRNA^{Thr} and its six single-point mutants, and analyzed them by PAGE under native and denaturing conditions. Wild-type hmtRNA^{Thr} and all mutants including one-nucleotide difference (ΔU60) migrated with the same rates on denaturing urea-PAGE (Figure 1B). On native PAGE, hmtRNA^{Thr}-G30A and -G70A migrated slightly but obviously slower compared with the wild-type hmtRNA^{Thr} (Figure 1B). These results suggested that the G30A and G70A mutations changed the conformation of hmtRNA^{Thr}. The structural alteration could be also detected using the melting temperature (T_m) value of tRNA. We compared the T_m value of wild-type hmtRNA^{Thr} and its various mutants, as shown in Figure 1C. Compared with the T_m value of wild-type hmtRNA^{Thr}, those of hmtRNA^{Thr}-G30A, -G70A and -A71G decreased by 23.5°C, 11°C and 5°C, respectively; however that of hmtRNA^{Thr}-A38G increased by 4.5°C; and those of hmtRNA^{Thr}-ΔU60 and -A39G showed no obvious change. The data showed that the G30A and G70A mutations decreased the stability of hmtRNA^{Thr} markedly, and correlated with the migration assay on native PAGE. The T_m value of hmtRNA^{Thr}-A38G mutant indicated a more rigid conformation.

The central role of tRNA is the generation of aminoacyl-tRNA, catalyzed by its cognate aminoacyl-tRNA synthetase, to supply the materials of protein biosynthesis. To understand the effect of these mutations on the charging capacity of hmtRNA^{Thr}, we performed aminoacylation of these hmtRNA^{Thr}s by hmThrRS. Four mutations (A39G, ΔU60, G70A and A71G) had little effect, whereas the G30A and A38G mutations caused an obvious decrease in the charging capacity of hmtRNA^{Thr} (Figure 1D). Fur-

ther aminoacylation kinetics of hmThrRS for the wild-type hmtRNA^{Thr}, hmtRNA^{Thr}-G30A and -A38G showed that the k_{cat} values for both hmtRNA^{Thr}-G30A and -A38G were decreased, while their K_m values were increased by ∼3-fold compared with that of hmtRNA^{Thr}. In addition, the catalytic efficiencies (k_{cat}/K_m) of hmThrRS for hmtRNA^{Thr}-G30A and -A38G were only 14% and 21% of that for hmtRNA^{Thr}, respectively (Table 1).

hmtRNA^{Thr}-G30A displayed alterations in shifting in the native gel and amino acid charging, and had a decreased T_m value. The A38G mutation, located in a critical loop region, reduced amino acid charging and increased the T_m value (in contrast to other mutations). The other four point mutations slightly influenced shifting in the native gel and the T_m value and had no or negligible effects on amino acid charging, suggesting they likely affected mitochondrial translation via different mechanisms in downstream steps (such as elongation factor binding, ribosome binding, or decoding). Therefore, we selected the G30A and A38G mutations to study the potential effects of mutations on the structure and functions of hmtRNA^{Thr}.

The G30–C40 base pair is essential for maintaining the anticodon stem structure of hmtRNA^{Thr} because of non-Watson–Crick base pair A29/C41

Interestingly, the middle of the anticodon stem of hmtRNA^{Thr} transcript has a non-Watson–Crick base pair, A29/C41 (Figure 2A). The severe effect of the G30A mutation on the local structure and function of hmtRNA^{Thr} suggested that, with a natural non-Watson–Crick A29/C41 base pair in the middle, the G30–C40 base pair in the stem should be crucial to maintain the structure of the anticodon stem and loop. Therefore, we constructed C40A, C40G, and C40U mutations to disrupt the G30–C40 Watson–Crick base pair; G30A/C40U to form A30–U40, a new Watson–Crick base pair; G30A/A29G with the G29-C41 Watson–Crick base pair, and A30–C40 non-Watson–Crick base pair in the context of the wild-type hmtRNA^{Thr} transcript (Figure 2A). Electrophoretic mobility results showed that the hmtRNA^{Thr}-C40A, -C40G, and -C40U mutants with a non-Watson–Crick base pair migrated more slowly than the wild-type hmtRNA^{Thr} and as slowly as hmtRNA^{Thr}-G30A (Supplementary Figure S1). However, the mutants hmtRNA^{Thr}-G30A/C40U with Watson–Crick base pair A30-U40 and hmtRNA^{Thr}-G30A/A29G with one Watson–Crick base pair G29-C41 and one non-Watson–Crick base pair A30-C40 migrated as fast as the wild-type hmtRNA^{Thr} (Supplementary Figure S1). Further, analysis of the T_m values showed that those of the hmtRNA^{Thr}-G30A, -C40A, -C40G and -C40U mutants were decreased markedly compared with that of the wild-type hmtRNA^{Thr} (Figure 2B). However, the T_m values of the hmtRNA^{Thr}-G30A/C40U and -G30A/A29G mutants were similar to that of the wild-type hmtRNA^{Thr} (Figure 2B). The data from the hmtRNA^{Thr}-G30A/A29G mutant suggested that the structurally detrimental effect of the G30A mutation was caused by the A29/C41 non-Watson–Crick base pair in hmtRNA^{Thr}. The results showed that at least one Watson–Crick base pair in the third and fourth base pairs of the anticodon stem is necessary to maintain the conformation of hmtRNA^{Thr}.

A nuclease probing assay was then carried out with unpaired G residues-specific RNase T1 and single-stranded specific RNase S1 to reveal the effect of the G30A mutation on the structure of hmtRNA^{Thr}. The results showed that the main RNase S1 cleavage sites were at positions 34 and 35 in the anticodon loop of the wild-type hmtRNA^{Thr} (Figure 3A and B). However, the RNase S1 cleavage sites for hmtRNA^{Thr}-G30A obviously shifted to positions 30 and 31 in the anticodon stem, suggesting that the G30A mutation disrupted the base pair between U31 and A39, and thus disturbed the stem structure (Figure 3A and B). The main RNase S1 cleavage site in hmtRNA^{Thr}-G30A/C40U shifted again to positions 34 and 35 (Figure 3A and B), indicating that the stem structure was rescued by an additional C40U mutation. A minor portion of hmtRNA^{Thr}-G30A/C40U was also digested at positions 30 and 31 (Figure 3A and B), suggesting that the weaker Watson–Crick base pair A30–U40 is less efficient in maintaining the stem structure compared with the stronger Watson–Crick base pair G30–C40 in hmtRNA^{Thr}. Our data showed that, at least from viewpoint of structure, the fourth base pair of the anticodon stem should be a Watson–Crick base pair (either G–C or A–U), even G–U was not tolerated (as shown by the decreased T_m of the hmtRNA^{Thr}-C40U mutant). Once the fourth base pair was disrupted, the local structure was altered; however, this could be compensated for by restoring the third Watson–Crick base pair of the stem (as illustrated by the hmtRNA^{Thr}-G30A/A29G mutant).

The G30A mutation influences tRNA binding and aminoacylation by hmThrRS

The above data clearly showed the critical role of G30–C40 in maintaining the local structure of the anticodon stem of hmtRNA^{Thr}. Whether the structural alteration in the anticodon stem influences its interaction with hmThrRS was not clear; therefore, we used biolayer interferometry (BLI) and immobilized hmThrRS on a sensor chip to detect the affinity between hmThrRS and hmtRNA^{Thr}. The results showed that the K_d value of hmThrRS for hmtRNA^{Thr}-G30A was 1.5-fold weaker than that for wild-type hmtRNA^{Thr} (Table 2). Similarly, the K_d values for both hmtRNA^{Thr}-C40A and -C40G were increased, showing that the affinity between hmThrRS and hmtRNA^{Thr} was weakened upon disrupting the G30–C40 base pair as hmtRNA^{Thr}-G30A mutant (Table 2). The K_d value for hmtRNA^{Thr}-C40U was slightly higher, indicating a weaker affinity to hmThrRS (Table 2). The affinities for hmtRNA^{Thr}-G30A/C40U and hmtRNA^{Thr}-G30A/A29G were comparable to that of the wild-type hmtRNA^{Thr} (Table 2). The above data suggested that the G30A mutation weakens the interaction between hmThrRS with hmtRNA^{Thr} by altering the conformation of the anticodon stem.

We next assayed and compared the aminoacylation activity of hmThrRS for hmtRNA^{Thr} and its mutants. The results showed that, among the mutants of C40, the tRNA charging level of hmtRNA^{Thr}-C40G was the most significantly decreased (Figure 4A), while those of the

Table 1. Aminoacylation kinetics of hmThrRS for various hmtRNA^{Thr} mutants

tRNA	k_{cat} (s^{-1})	K_m (mM)	k_{cat}/K_m ($\times 10^{-3}$)	Relative k_{cat}/K_m (%)
hmtRNA^{Thr}	0.09 ± 0.01	1.05 ± 0.01	86	100
-G30A	0.04 ± 0.003	3.37 ± 0.09	12	14
-C40A	0.06 ± 0.004	4.85 ± 0.3	12	14
-C40U	0.08 ± 0.005	3.65 ± 0.2	22	26
-C40G	0.03 ± 0.001	2.95 ± 0.4	10	12
-G30A/A29G	0.11 ± 0.03	1.40 ± 0.03	95	110
-G30A/C40U	0.13 ± 0.05	1.36 ± 0.03	96	111
-A38G	0.05 ± 0.007	2.81 ± 0.2	18	21
-A38C	0.07 ± 0.005	2.24 ± 0.03	31	36
-A38U	0.08 ± 0.005	3.92 ± 0.1	20	23

The results represent the average of at least two independent trials with the standard deviations indicated.

A

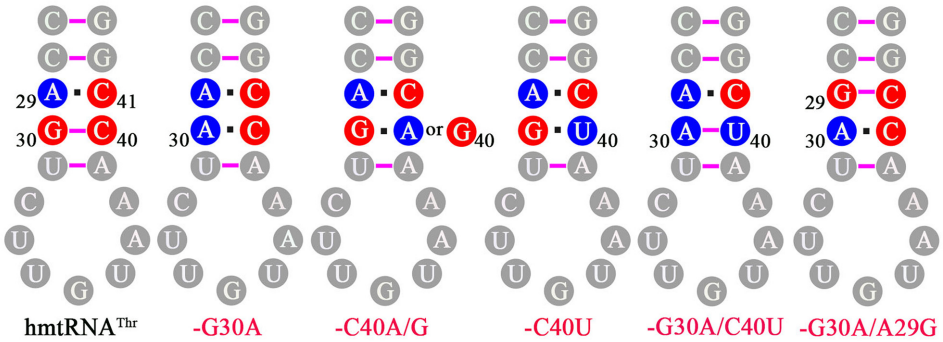

B

Table. Thermal stability of hmtRNA^{Thr} mutants

tRNA	T_m (°C)
hmtRNA^{Thr}	53.5 ± 0.3
-G30A	30.0 ± 0.1
-C40A	37.5 ± 0.4
-C40G	33.5 ± 0.2
-C40U	40.5 ± 0.2
-G30A/C40U	52.5 ± 0.2
-G30A/A29G	52.0 ± 0.3

Figure 2. G30-C40 base pair is essential for hmtRNA^{Thr} stability. (**A**) Anticodon loop and stem structure of hmtRNA^{Thr} and its mutations. (**B**) T_m values of hmtRNA^{Thr} mutants.

Table 2. Binding affinities of hmThrRS or *Sc*Qri7 with various hmtRNA^{Thr} mutants

hmThrRS K_d (μM)	tRNA	*Sc*Qri7 K_d (nM)
1.8 ± 0.3	hmtRNA^{Thr}	26.9 ± 1.2
3.1 ± 0.4	-G30A	4.1 ± 0.2
4.3 ± 0.3	-C40A	11.8 ± 0.5
2.4 ± 0.1	-C40U	11.0 ± 0.3
3.6 ± 0.2	-C40G	3.3 ± 0.1
1.6 ± 0.2	-G30A/C40U	25.5 ± 1.0
1.4 ± 0.4	-G30A/A29G	29.1 ± 2.1
2.3 ± 0.1	-A38G	31.2 ± 1.9
3.7 ± 0.2	-A38C	51.7 ± 1.6
4.3 ± 0.4	-A38U	47.4 ± 1.1

The results represent the average of at least two independent trials with the standard deviations indicated.

hmtRNA^{Thr}-C40A and -C40U mutants were comparable to that of hmtRNA^{Thr}-G30A, indicating that G40 was most unfavorable at this site. However, the charging levels of hmtRNA^{Thr}-G30A/C40U and -G30A/A29G were rescued to that of the wild-type hmtRNA^{Thr} (Figure 4A). These results suggested that disruption of the G30–C40 base pair caused the reduction in the aminoacylation level (Figure 4A), which otherwise could be restored by re-forming the G29–C41 base pair. Further analysis of the aminoacylation kinetics showed that the K_m values of hmThrRS for all hmtRNA^{Thr}-C40A, -C40U, and -C40G mutants were increased by 3–5-fold, with a decreased k_{cat}. The catalytic efficiencies of hmThrRS for the three mutants were only 14%, 26%, and 12% of that for hmtRNA^{Thr}, respectively (Table 1). However, both the K_m and k_{cat} values for the double-

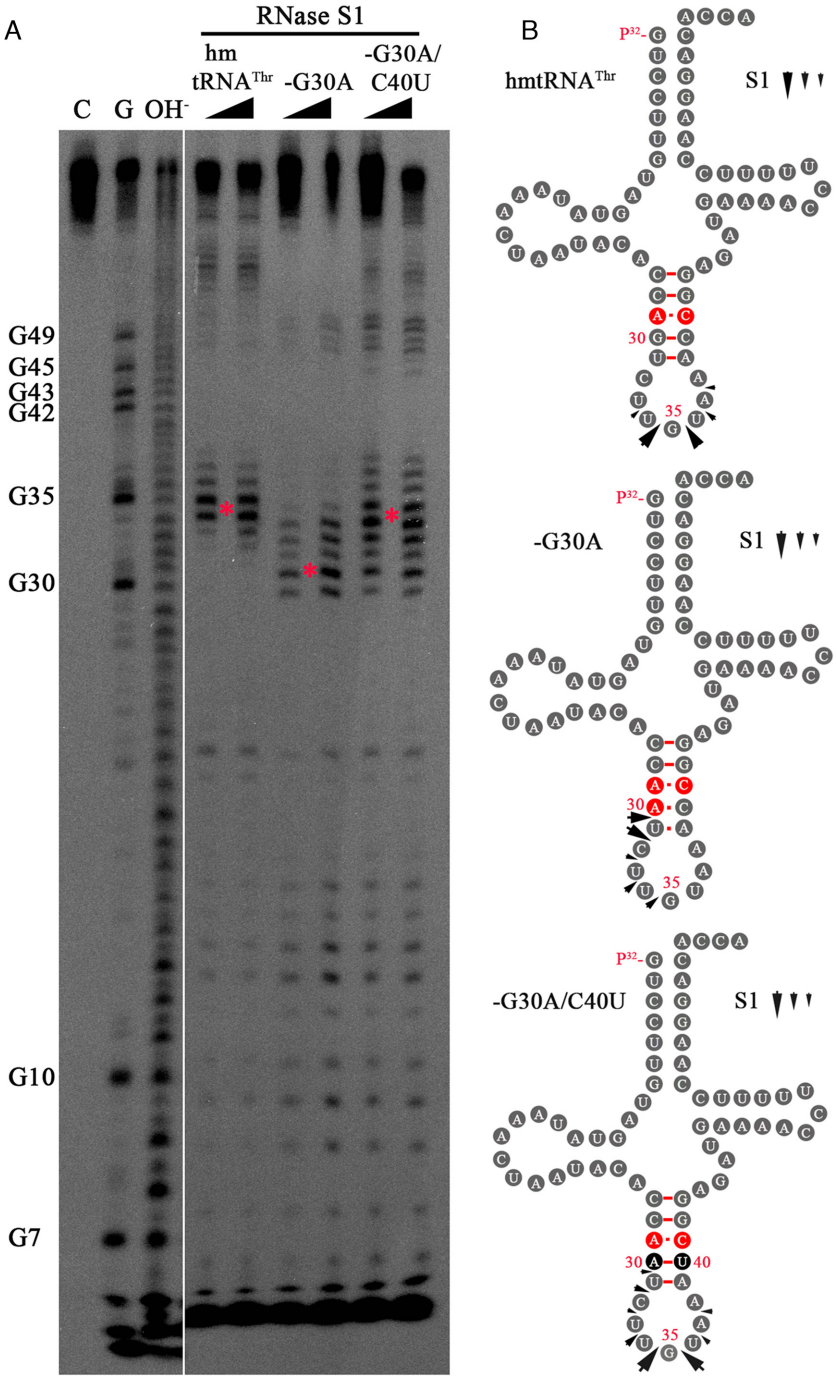

Figure 3. Enzymatic probing analysis of hmtRNA^{Thr}, -G30A and -G30A/C40U. (**A**) Probing was performed using various RNase S1 concentrations. Lane C, control; lane G, ladder digested by RNase T1 under denaturing conditions; lane OH^-, alkaline digestion. (**B**) Structure analysis by enzymatic probing. The red stars indicate the main RNase S1 cleavage sites.

site mutants, hmtRNA^{Thr}-G30A/C40U and -G30A/A29G, were similar to those of the wild-type hmtRNA^{Thr} (Table 1); thus, the catalytic efficiency of hmThrRS was not affected by the double-site mutations. Altogether, the above data revealed that the G30A mutation of hmtRNA^{Thr} decreases the affinity between hmThrRS and hmtRNA^{Thr} by disrupting the G30–C40 Watson–Crick base pair of hmtRNA^{Thr}, which could be compensated for by a Watson–Crick base pair G29–C41. In the third and fourth base pairs of the anticodon stem of hmtRNA^{Thr}, at least one Watson–Crick base pair is necessary to maintain the structure of the anticodon stem and loop. It also suggested that the conformation, but not the nucleotide sequence, in the anticodon stem determines the proper recognition by hmThrRS, because hmtRNA^{Thr}-G30A/C40U and -G30A/A29G are well qualified as hmtRNA^{Thr}.

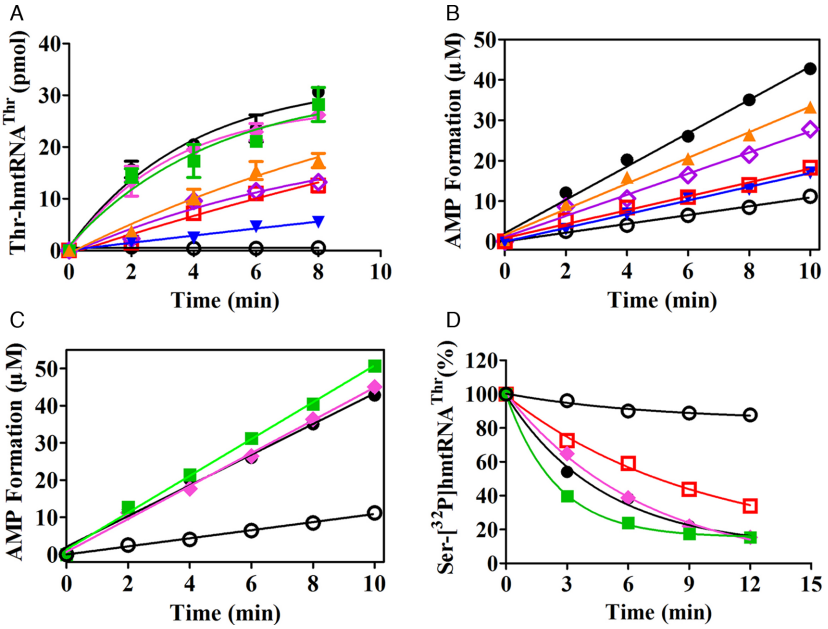

Figure 4. Aminoacylation and editing properties of hmThrRS for hmtRNA^{Thr}-G30A. (**A**) Aminoacylation of hmtRNA^{Thr} (●), -G30A (□), -C40A (◇), -C40U (▲), -C40G (▼), -G30A/C40U (◆) and -G30A/A29G (■) catalyzed by hmThrRS, without enzyme addition as a control (○). (**B**) AMP formation by hmThrRS in the presence of hmtRNA^{Thr} (●) or its mutants hmtRNA^{Thr}-G30A (□), -C40A (◇), -C40U (▲), -C40G (▼), without tRNA addition as a control (○). (**C**) AMP formation by hmThrRS in the presence of hmtRNA^{Thr}-G30A/C40U (◆) or -G30A/A29G (■) mutant, without tRNA addition as a control (○). (D) Post-transfer editing of hmThrRS for mischarged hmtRNA^{Thr} (●) or its mutants hmtRNA^{Thr}-G30A (□), -G30A/C40U (◆) and -G30A/A29G (■), without enzyme addition as a control (○). Error bars indicate the standard deviations.

Disrupting the G30–C40 Watson–Crick pair induces a decrease in editing by hmThrRS

hmThrRS contains an editing domain to deacylate mischarged tRNA and ensure the fidelity of protein synthesis. As stated previously, hmThrRS clears mis-acylated Ser-tRNA^{Thr} via its post-transfer editing function, whose abolition resulted in generation of Ser-tRNA^{Thr} (29). In addition, tRNA functions as a stimulator to promote tRNA-dependent pre-transfer editing. To investigate whether the G30A mutation affected the editing function of hmThrRS, we performed Ser-included AMP formation assays (measuring the total editing function, including tRNA-independent, tRNA-dependent pre-transfer editing, and post-transfer editing) in the absence or presence of hmtRNA^{Thr} or the hmtRNA^{Thr}-G30A mutant. The results showed that the AMP formation in the presence of hmtRNA^{Thr}-G30A decreased significantly compared with that of hmtRNA^{Thr} (Figure 4B). The observed AMP formation rate constant (k_{obs}) in the presence of hmtRNA^{Thr}-G30A was only 43% of that in the presence of hmtRNA^{Thr} (Table 3). To explore whether the editing-impairment was due to structural alteration of the anticodon stem, we performed AMP formation assays in the presence of hmtRNA^{Thr}-C40A, -C40G, and -C40U. The results showed that the k_{obs} values decreased to different extents (Figure 4B and Table 3). However, the double-site mutants, hmtRNA^{Thr}-G30A/C40U and -G30A/A29G, did not affect the total editing activity of hmThrRS (Figure 4C and Table 3), again suggesting the importance of at least one Watson–Crick base pair at 30–40 and 29–41 for the correct structure of hmtRNA^{Thr} and the editing function of hmThrRS. In addition, the results of a deacylation assay showed that the post-transfer editing activity of hmThrRS for hmtRNA^{Thr}-G30A was slightly decreased compared with that of the wild-type hmtRNA^{Thr}, while the double-site mutations G30A/C40U and G30A/A29G in hmtRNA^{Thr} did not affected the post-transfer editing activity of hmThrRS (Figure 4D).

Table 3. Observed rate constants of AMP formation by hmThrRS with Ser in the presence of wild-type hmtRNA^{Thr} or its mutants

tRNA	$k_{obs} \times 10^{-3}(s^{-1})$	Relative k_{obs} (%)
hmtRNA^{Thr}	33.3 ± 0.6	100
-G30A	14.5 ± 0.4	43
-C40A	20.1 ± 0.1	60
-C40U	26.3 ± 0.6	79
-C40G	15.1 ± 0.3	45
-G30A/A29G	34.2 ± 0.6	103
-G30A/C40U	36.3 ± 1.7	109
-A38G	16.8 ± 0.6	50
-A38C	20.6 ± 0.3	61
-A38U	19.9 ± 0.3	60

The results represent the average of two independent trials with the standard deviations indicated.

G30A mutation in bmtRNA^{Thr} has little effect on its functions because of its natural G29–C41 base pair

Interestingly, bmtRNA^{Thr} is similar to hmtRNA^{Thr} in sequence and structure in the anticodon stem, except for a Watson–Crick base pair, G29–C41 (Figure 5A). We constructed the G30A mutation in bmtRNA^{Thr} and

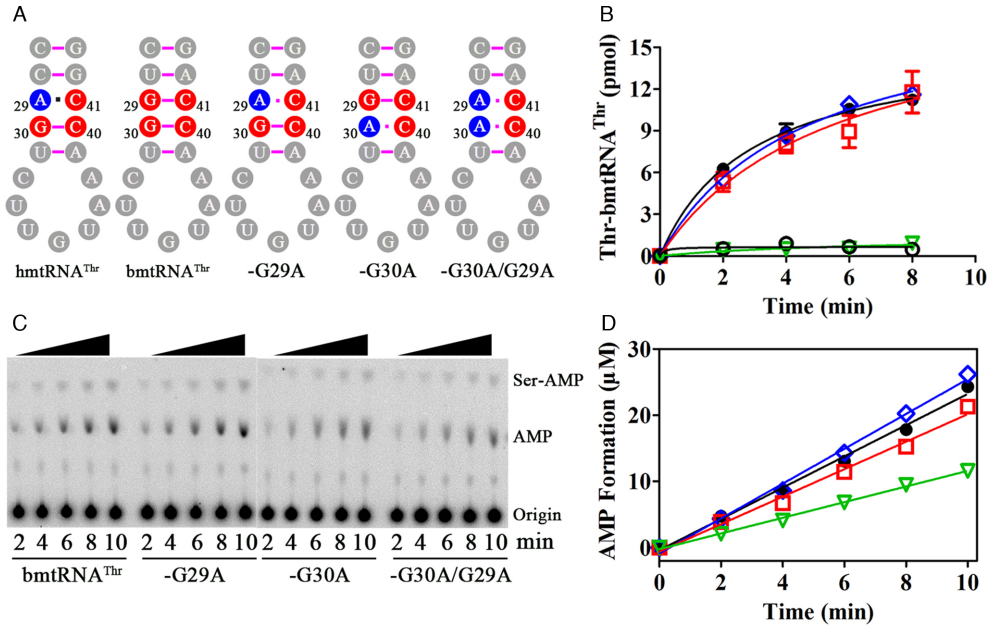

Figure 5. Disrupting the G30-C40 base pair of bmtRNA^{Thr} does not affect the aminoacylation and editing properties of hmThrRS. (**A**) Anticodon stem and loop structure of hmtRNA^{Thr}, bmtRNA^{Thr}, and its mutants. (B) Aminoacylation of bmtRNA^{Thr} (●) and its mutants bmtRNA^{Thr}-G30A (□), -G29A (◇) and -G30A/G29A (▽) catalyzed by hmThrRS, without enzyme addition as a control (○). (**C**) AMP formation of hmThrRS in the presence of bmtRNA^{Thr} or its mutants. (**D**) Graphic representations of AMP formation in (C), bmtRNA^{Thr} (●), -G30A (□), -G29A (◇) and -G30A/G29A (▽). Error bars indicate the standard deviations.

measured the accepting activity of bmtRNA^{Thr}-G30A. The data showed that the bmtRNA^{Thr}-G30A mutant had a comparable aminoacylation level to bmtRNA^{Thr} (Figure 5B), which was different from the obvious decreased activity of hmtRNA^{Thr}-G30A (Figure 4A). To reveal the potential importance of the G29–C41 base pair of mtRNA^{Thr}, we further constructed bmtRNA^{Thr}-G29A and -G30A/G29A mutants to mimic hmtRNA^{Thr} and the hmtRNA^{Thr}-G30A mutant (Figure 5A). The results showed that bmtRNA^{Thr}-G30A/G29A lost its accepting activity (Figure 5B), which was consistent with that of the G30A mutation in hmtRNA^{Thr}. Meanwhile, bmtRNA^{Thr}-G29A had little effect on the charging activity (Figure 5B). Furthermore, we performed an AMP formation assay to detect whether these bmtRNA^{Thr} mutations affected the editing properties of hmThrRS. The data showed that among the mutants, only the double-site mutant bmtRNA^{Thr}-G30A/G29A decreased the editing activity of hmThrRS (Figure 5C and D). Our results further indicated that at least one Watson–Crick base pair in the third and fourth base pairs of the anticodon stem is crucial for aminoacylation and the editing activities for mitochondrial tRNA^{Thr}; if these two base pairs were non-Watson–Crick base pairs, the functions of mtRNA^{Thr} would be disrupted.

The G30A mutation in hmtRNA^{Trp} causes structure fragility, which arises from a natural A29/C41 non-Watson–Crick base pair

By analyzing the secondary structure of all human mitochondrial tRNAs, we found that besides hmtRNA^{Thr}, only hmtRNA^{Trp} has a natural A29/C41 non-Watson–Crick base pair (Figure 6A). The electrophoretic mobility results showed that hmtRNA^{Trp}-G30A also migrated slower than hmtRNA^{Trp} in a native gel (Supplementary Figure S2), which could be rescued by restoring the G29–C41 base pair, because hmtRNA^{Trp}-G30A/A29G migrated as fast as hmtRNA^{Trp} (Supplementary Figure S2). Furthermore, the T_m value of the hmtRNA^{Trp}-G30A mutant was markedly decreased and similarly rescued by a further A29G mutation, as shown for the double-site mutant hmtRNA^{Trp}-G30A/A29G (Figure 6B). The above results clearly showed that the natural A29/C41 non-Watson–Crick base pair made the structure of hmtRNA^{Trp} sensitive to the G30A mutation, similar to the case in hmtRNA^{Thr}. We also investigated the effect of the G30A mutation on the Trp-accepting capacity mediated by the purified recombinant human mitochondrial tryptophanyl-tRNA synthetase (hmTrpRS) (Figure 6C). The G30A mutation did not affect the aminoacylation of hmtRNA^{Trp} (Figure 6D), implying that hmtRNA^{Trp} recognition by hmTrpRS was not reliant on the anticodon stem. The above data confirmed that the structural integrity of hmtRNA^{Trp} was also dependent on the G30–C40 base pair because of a natural A29/C41 non-Watson–Crick base pair. Indeed, the m. 5540 G>A (hmtRNA^{Trp} G30A) mutation is associated with a progressive encephalopathy and cytochrome c oxidase deficiency (37).

A38 is an important element for hmtRNA^{Thr} charging, the interaction of hmThrRS and hmtRNA^{Thr}, and the editing function of hmThrRS

Besides the G30A mutation, the A38G mutation also impaired the tRNA charging capacity in the initial screening assays (Figure 1C), implying that A38, in the anticodon

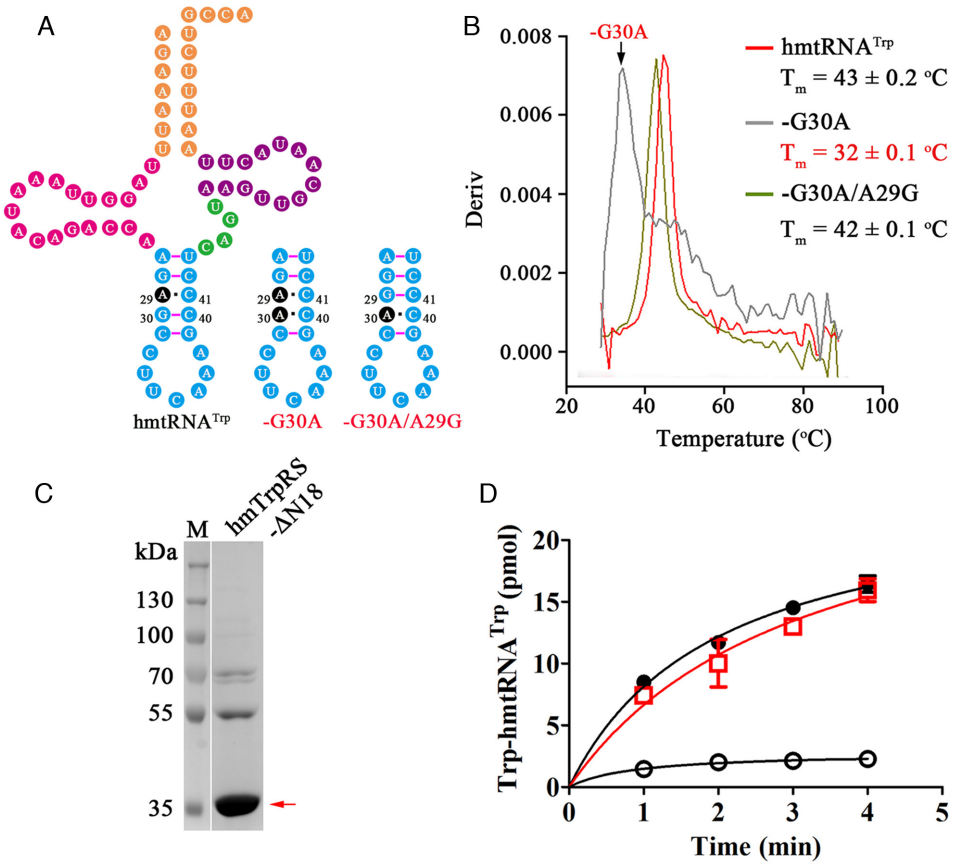

Figure 6. The G30A mutation causes structural flexibility of hmtRNA^{Trp}. (**A**) Cloverleaf structure of hmtRNA^{Trp} and its mutants. (**B**) Temperature curves of hmtRNA^{Trp} and its mutants measured at 260 nm. (**C**) Analysis of purified mature hmTrpRS. (D) Aminoacylation levels of hmtRNA^{Trp} (●) and -G30A (□) catalyzed by hmTrpRS, without enzyme addition as a control (○). Error bars indicate the standard deviations.

loop, is a potentially key element in aminoacylation. We changed A38 to C or U, obtaining hmtRNA^{Thr}-A38C or -A38U. A time-course curve of the aminoacylation reaction showed that the Thr-accepting ability of all the substitution mutants of hmtRNA^{Thr}-A38C, -A38U, and -A38G obviously decreased compared with that of hmtRNA^{Thr} (Figure 7A). Furthermore, the aminoacylation kinetic parameters showed that the K_m values of hmThrRS for the hmtRNA^{Thr}-A38C, -A38U and -A38G mutants increased by about 3-fold compared with that of hmtRNA^{Thr}, while the k_{cat} values for the three mutants decreased slightly (Table 1). The catalytic efficiencies for hmtRNA^{Thr}-A38C, -A38U and -A38G were 36%, 23%, and 21% of that of hmtRNA^{Thr}, respectively (Table 1). Furthermore, the affinities between hmThrRS and hmtRNA^{Thr} or hmtRNA^{Thr}-A38C, -A38U and -A38G mutants were also measured and compared using BLI. The data showed that the K_d value of hmThrRS for hmtRNA^{Thr}-A38G was comparable to that for hmtRNA^{Thr}, while the K_d values for hmtRNA^{Thr}-A38C and -A38U increased by ∼2-fold (Table 2). In addition, we performed the AMP formation assays to investigate the role of A38 in the editing function of hmThrRS. The results showed that the AMP formation with hmtRNA^{Thr}-A38G decreased markedly compared with that of hmtRNA^{Thr} (Figure 7B). The k_{obs} of hmThrRS for hmtRNA^{Thr}-A38G were only 50% of that for hmtRNA^{Thr} (Table 3). Similarly, both hmtRNA^{Thr}-A38C and -A38U resulted in a reduction in AMP formation (Figure 7B, Table 3). Moreover, the results from the deacylation assay of Ser-tRNA^{Thr} showed that among the three mutants, hmtRNA^{Thr}-A38G led to a marked decrease in the post-transfer editing activity of hmThrRS (Figure 7C). The above data indicated that A38 plays an important role in hmtRNA^{Thr}/hmThrRS interactions, tRNA recognition, and editing properties of hmThrRS.

G30A and A38G mutations induce a marked decrease in t^{6}A modification in hmtRNA^{Thr}

tRNA modification is a crucial step in the tRNA life cycle, and contributes to its structure and function. Defects in tRNA modification frequently result in mitochondrial diseases (10,38). Whether the pathogenic mutations G30A and A38G of hmtRNA^{Thr} affected modifications of hmtRNA^{Thr} was unknown. Although the complete post-transcriptional modification pattern of hmtRNA^{Thr} has not been reported, post-transcriptional modifications in bmtRNA^{Thr} have been determined, including m^{1}A9, m^{3}C32, t^{6}A37, Ψ67 and m^{5}C72 (39). We proposed that hmtRNA^{Thr} probably had a similar modification pattern to bmtRNA^{Thr}, except for Ψ67, because A67 is present in hmtRNA^{Thr}. The t^{6}A modification at position 37 aroused

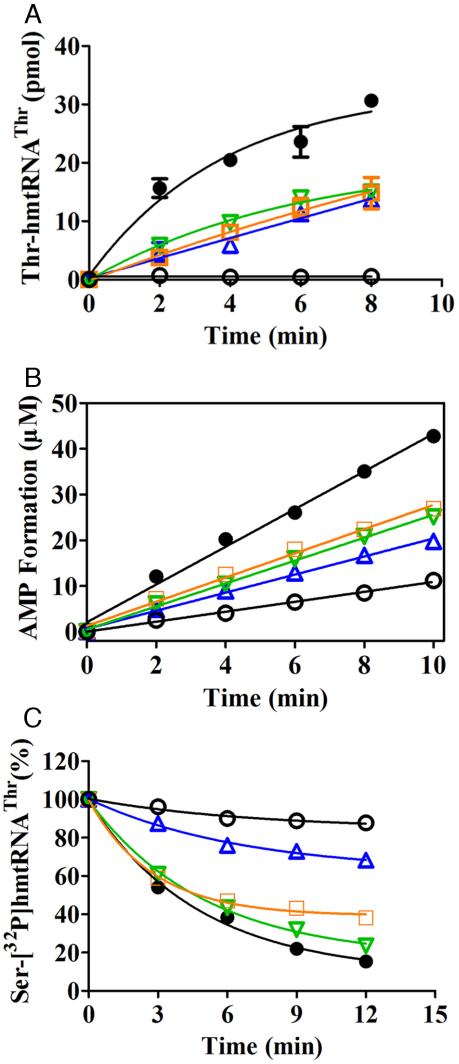

Figure 7. A38 is a key element for tRNA charging and editing of hmThrRS. (**A**) Aminoacylation levels of hmtRNA^{Thr} (●) and its mutants hmtRNA^{Thr}-A38G (△), -A38C (▽) and -A38U (□) catalyzed by hmThrRS, without enzyme addition as a control (○). (**B**) Quantification of AMP formation in the presence of hmtRNA^{Thr} (●), -A38G (△), -A38C (▽) or -A38U (□), without tRNA addition as a control (○). (**C**) Post-transfer editing of hmThrRS for mischarged hmtRNA^{Thr} (●), -A38G (△), -A38C (▽) and -A38U (□), without enzyme addition as a control(○). Error bars indicate the standard deviations.

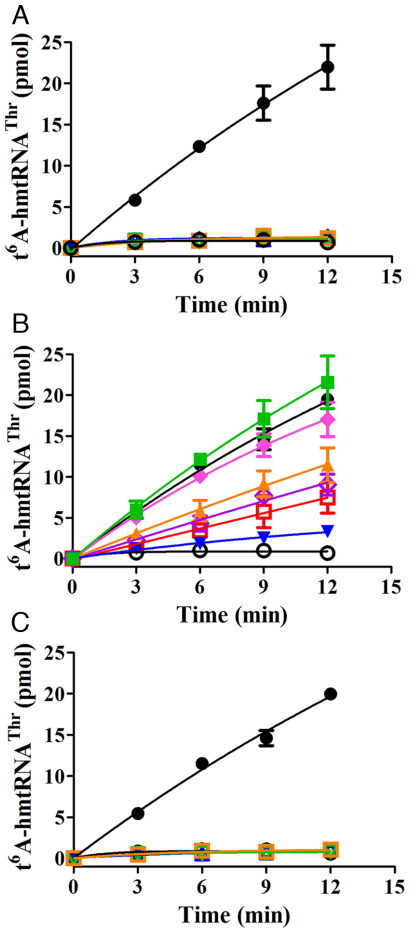

Figure 8. Both the G30A and A38G mutations cause decreased t^{6}A37 modification. (**A**) t^{6}A modification of hmtRNA^{Thr} (●), -A37G (△), -A37C (▽) and -A37U (□) mutants, without enzyme addition as a control (○). (**B**) t^{6}A biosynthesis of hmtRNA^{Thr} (●) and its mutants hmtRNA^{Thr}-G30A (□), -C40A (◇), -C40U (▲), -C40G (▼), -G30A/C40U (◆) and -G30A/A29G (■) catalyzed by *Sc*Sua5 and *Sc*Qri7, without enzyme addition as a control (○). (**C**) t^{6}A modification levels of hmtRNA^{Thr} (●), -A38G (△), -A38C (▽) and -A38U (□) mutants, without enzyme addition as a control (○). Error bars indicate the standard deviations.

our interest for the following reasons. First, G30A and A38G are close to A37. Second, the t^{6}A37 modification is essential to maintain the correct conformation of the anticodon loop (24,40). Third, in *Saccharomyces cerevisiae*, the enzymes *Sc*Sua5 and *Sc*Qri7 catalyze the t^{6}A modification at position 37 of tRNAs (27). Therefore, whether the t^{6}A modification in human tRNAs can be catalyzed by these two enzymes and whether this modification exists in hmtRNA^{Thr} need to be investigated. We purified *Sc*Sua5 and *Sc*Qri7 and showed that *Sc*Sua5/*Sc*Qri7 could catalyze the t^{6}A modification of hmtRNA^{Thr} efficiently (Figure 8A). To confirm that the t^{6}A modification occurs at position A37, we mutated A37 to C, G and U, respectively. Under the same conditions, t^{6}A could not be detected in the three substitutions of A37 (Figure 8A), indicating the t^{6}A37 also exists in hmtRNA^{Thr}, as in bmtRNA^{Thr}. However, the t^{6}A modification level of hmtRNA^{Thr}-G30A was significantly decreased compared with that of hmtRNA^{Thr} (Figure 8B). The observed rate constant (k_{obs}) of the t^{6}A modification in the hmtRNA^{Thr}-G30A was only 41% of that of hmtRNA^{Thr} (Table 4). As described above, three substitutions of another base for C40 in the anticodon stem decreased the thermal stability of these tRNAs (Figure 2C); and the t^{6}A modifications of hmtRNA^{Thr}-C40A, -C40U and -C40G were also decreased (Figure 8B and Table 4). However, the two double-site mutants, hmtRNA^{Thr}-G30A/C40U and -G30A/A29G, had similar t^{6}A modification levels compared with hmtRNA^{Thr}, because of the presence of one Watson–Crick base pair in the third and fourth base pairs in the anticodon stem (Figure 8B and Table 4). *Sc*Sua5/*Sc*Qri7 de-

Table 4. Observed rate constants of t^6A modification in wild-type $hmtRNA^{Thr}$ or its mutants by *Sc*Sua5/*Sc*Qri7

tRNA	$k_{obs} \times 10^{-3}(min^{-1})$	Relative k_{obs} (%)
$hmtRNA^{Thr}$	34.6 ± 0.1	100
-G30A	14.2 ± 1.9	41
-C40A	16.7 ± 0.7	48
-C40U	20.6 ± 1.3	60
-C40G	5.7 ± 0.3	16
-G30A/A29G	38.6 ± 1.9	111
-G30A/C40U	29.5 ± 1.7	85

The results represent the average of two independent trials with the standard deviations indicated.

creased the modification of t^6A in $hmtRNA^{Thr}$-G30A with lowest T_m. The above data showed that the t^6A modification occurs at position 37 of $hmtRNA^{Thr}$ and is associated with the stability of its anticodon stem. In addition, we found that the t^6A modification has a negligible (or a slightly inhibitory) effect on its aminoacylation (Supplementary Figure S3).

We also measured the t^6A modification level of $hmtRNA^{Thr}$-A38G. The data showed that the A38G mutation abolished the t^6A modification (Figure 8C). Further, we found that both the A38C and A38U mutations abolished the t^6A modification (Figure 8C). These results revealed that, on the one hand, A38 is a critical determinant for the t^6A modification in human mitochondrial tRNAs, at least for $hmtRNA^{Thr}$; and on the other hand, abolition of the t^6A37 modification of $hmtRNA^{Thr}$ is also likely to contribute to the pathogenesis of the A38G mutation.

G30A and A38G mutations alter the interaction between *Sc*Qri7 and $hmtRNA^{Thr}$

In the t^6A modification reaction, *Sc*Sua5 catalyzes the first step of TCA intermediate formation; *Sc*Qri7 catalyzes the second step, involving binding TCA and the tRNA substrate to form t^6A (27). To explore whether the mutations affected the affinity between *Sc*Qri7 and $hmtRNA^{Thr}$, we measured the K_d values of *Sc*Qri7 to $hmtRNA^{Thr}$ and its mutants using BLI. The K_d value of *Sc*Qri7 with $hmtRNA^{Thr}$ was 26.9 ± 1.2 nM, and with $hmtRNA^{Thr}$-G30A was 4.1 ± 0.2 nM, indicating that the affinity of the enzyme for the $hmtRNA^{Thr}$-G30A mutant was 6-fold stronger than that to $hmtRNA^{Thr}$ (Table 2). In addition, the K_d values of *Sc*Qri7 to all $hmtRNA^{Thr}$-C40 mutants, $hmtRNA^{Thr}$-C40A, -C40U and -C40G, were markedly decreased compared with that to $hmtRNA^{Thr}$ (Table 2), indicating a stronger affinity between the enzyme and $hmtRNA^{Thr}$ after alteration in structure of the anticodon stem. However, the K_d values of $hmtRNA^{Thr}$-G30A/C40U in which the fourth base pair in the stem is a Watson–Crick base pair and $hmtRNA^{Thr}$-G30A/A29G, in which the third is a Watson–Crick base pair, were similar to that of $hmtRNA^{Thr}$ (Table 2), again indicating the critical role of an intact stem structure in the proper interaction between *Sc*Qri7 and $hmtRNA^{Thr}$. Moreover, only a moderately weakened affinity of *Sc*Qri7 to $hmtRNA^{Thr}$-A38G was determined (Table 2); while those to $hmtRNA^{Thr}$-A38C and -A38U were ∼2-fold weaker than that to $hmtRNA^{Thr}$ (Table 2). Our data indicated that the rigid structure controlled by the third or fourth Watson–Crick base pair in the anticodon stem, and A38 in anticodon loop, are important elements for the interaction between *Sc*Qri7 and $hmtRNA^{Thr}$, and for the t^6A37 modification.

DISCUSSION

We further expanded the sequences with a broader species spectrum from thirteen eukaryotes including primates, mammals, non-mammalian vertebrates, and invertebrate. Their evolutionary relationship was constructed based on divergence times calculated by Timetree (Supplementary Figure S4A) (41). Detailed analysis of the sequences of the anticodon stem showed that the third base pair is always a Watson–Crick pair in the $mtRNA^{Thr}$s from invertebrate, non-mammalian vertebrates, mammals, and primates, except for gorilla and human $mtRNA^{Thr}$s (Supplementary Figure S4B), suggesting that the gain of A29/C41 non-Watson–Crick base pair in gorilla and human $mtRNA^{Thr}$s is a later evolutionary event. The fourth base pair (G30–C40) is highly conserved in all $mtRNA^{Thr}$s (Supplementary Figure S4B). In addition, the second base pair is U28-A42 in some lower eukaryotes, which is different to the C28–G42 in $hmtRNA^{Thr}$. We found that the C28U/G42A mutation had no effect on $hmtRNA^{Thr}$ migration, thermal stability, and aminoacylation (data not shown). Thus, we hypothesized that the A29/C41 mismatch is a newly evolved non-Watson–Crick pair in mitochondrial $tRNA^{Thr}$s from *Gorilla gorilla* and *Homo sapiens*, while a Watson–Crick base pair is present in those from other representative eukaryotes (this work) or in lower eukaryotes, such as *Saccharomyces cerevisiae* and *Schizosaccharomyces pombe* (42). All nucleotides in the anticodon stem, particularly the last three base pairs, have been suggested to be critical for a proper helical conformation during genetic code decoding (43). Therefore, it is reasonable that the introduction of the A29/C41 non-Watson–Crick base pair in $hmtRNA^{Thr}$ highlights the essential role of the downstream strong G30–C40 base pair in regulating tRNA structure and functions. The T_m value of $hmtRNA^{Thr}$ with A30–U40 was much larger than that of tRNA with the G30–U40 wobble base pair, suggesting that G30–U40 is less stable than A30–U40, at least in these positions. Consistently, both aminoacylation and editing activities at the presence of $hmtRNA^{Thr}$ with G30-U40 were reduced, possibly because of lower stability and/or the altered pit of the anticodon stem helix with G30–U40. Mutations causing two mismatches at 29/41 and 30/40 positions would impair the structural integrity and have a direct influence on various functional steps during the tRNA life cycle. Consistently, the detrimental effect of the mismatch between bases 29 and 41 in $hmtRNA^{Trp}$ makes it very sensitive to local mutations leading to a mismatch between 30 and 40 bases. In fact, the $hmtRNA^{Trp}$ G30A mutation leads to syndromes with a progressive encephalopathy and cytochrome c oxidase deficiency (37), probably because of an altered tRNA structure in the anticodon stem. The presence of a Watson–Crick pair between bases 29 and 41 in mitochondrial $tRNA^{Thr}$s from other species suggested that these tRNAs are also tolerant to the single-point mutation disrupting the G29–C41 or G30–C40

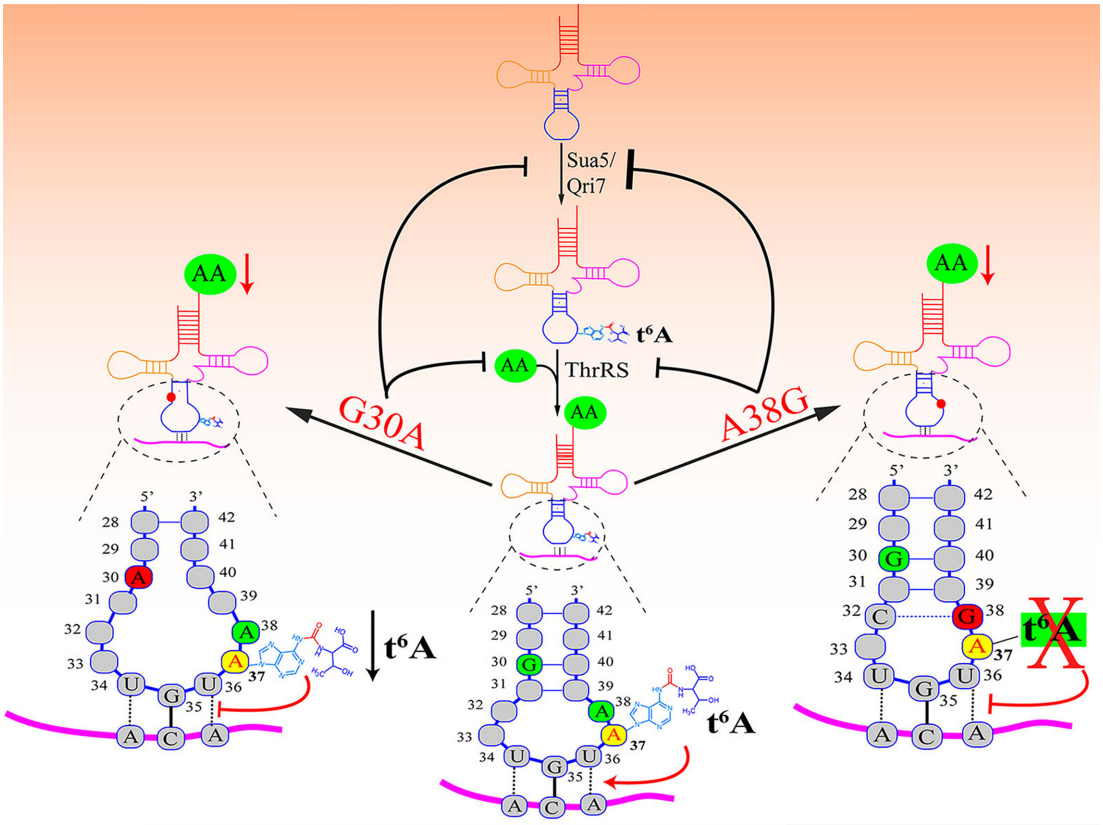

Figure 9. Model for the potential pathogenic mechanism of G30A and A38G mutations in hmtRNA^{Thr}. In human mitochondria, the hmtRNA^{Thr} transcript was modified, including the t^{6}A modification; the fully modified hmtRNA^{Thr} was charged with Thr by hmThrRS with the resultant Thr-hmtRNA^{Thr} transferred to the mitochondrial ribosome for protein synthesis. The G30A mutation decreased the aminoacylation and editing activities of hmThrRS and the t^{6}A modification level by disrupting the crucial G30–C40 base pair and thus altering the helical conformation of hmtRNA^{Thr}. The A38G mutation decreased the aminoacylation and editing of hmThrRS and, importantly, abolished the synthesis of t^{6}A37, possibly forming a strong C32–G38 base pair. Decreased aminoacylation, editing, and downregulated or abolished t^{6}A37 formation, which is critical for stabilizing the codon-anticodon interaction, separately or collectively had detrimental effects on the speed, accuracy, and/or fidelity of the genetic code flow in human mitochondria. Other effects of the mutations on the tRNA functions (such as other modifications, interaction with the ribosome, etc.) may also contribute to the observed pathogenesis.

base pairs, as revealed in bmtRNA^{Thr}. The evolutionary advantage and possible role of the newly acquired A29/C41 non-Watson–Crick base pair is not clear. One possibility is that the introduced A29/C41 non-Watson–Crick base pair might fine-tune the flexibility of the anticodon stem of mtRNA^{Thr}s from Gorillas and humans, and contribute to its mRNA decoding capacity on mitochondrial ribosomes.

Recently, the general sequence features near the anticodon stem and loop based on 400 elongator tRNAs from bacteria, eukaryotes and archaea have been summarized (43). hmtRNA^{Thr} exhibits both conservation and divergence from canonical tRNAs in the anticodon stem. Interesting, despite only Watson–Crick base pairs being tolerated between bases 29–41, hmtRNA^{Thr} has evolved the A29/C41 non-Watson–Crick pair, which subsequently makes the G30–C40 base pair extremely sensitive to non-Watson–Crick mutations (43). Indeed, once a Watson–Crick base pair is re-formed between bases 29 and 41, this sensitivity of the G30–C40 base pair is relieved. Lastly, the nucleotide at position 31 of tRNAs prefer A>C>G>>U (43); however, hmtRNA^{Thr} has U31, leading to A39, but not G39 or ψ39, starting the helical stem (43).

The anticodon stem of *Saccharomyces cerevisiae* mitochondrial tRNA^{Thr} (*Sc*mtRNA^{Thr}) is an important element for the binding and catalysis of *Sc*mThrRS to *Sc*mtRNA^{Thr} (44). The identity nucleotides in tRNA^{Thr} from *E. coli*, *S. cerevisiae*, and *T. thermophilus* have been reported, including G1-C72, C2-G71, U3-A70, G34, U35, G36 and (or) U73 (45–49). Our previous study showed that G35 and U36 were the identity determinants in hmtRNA^{Thr} (29). Based on the data in the present work, we suggested that G30 is important in maintaining a proper conformation of anticodon stem and that A38 is a key element for tRNA aminoacylation and editing.

The t^{6}A modification strengthens the codon-anticodon pairing and facilitates translational fidelity (24,25). The presence of a t^{6}A modification in bmtRNA^{Thr} strongly suggested that it also exists in hmtRNA^{Thr}. Our results showed that hmtRNA^{Thr} could be t^{6}A37-modified. The G30A mutation resulted in marked reduction in the t^{6}A modification, which could be rescued by G30A/C40U or G30A/A29G mutations, implying the importance of the intact structure of the anticodon stem in t^{6}A modification. hmtRNA^{Thr} (anticodon UGU) belongs to the intermediate group of decoding tRNAs because the codon box contains a weak A1–U36

pair in the first position (43). The t^6A modification is essential to stabilize the weak codon-anticodon pair A1–U36 and avoid miscoding in the codon boxes (43). Defects of the t^6A modification often lead to an increased frequency of frameshift events (26,50). Therefore, the G30A mutation in the anticodon stem of $hmtRNA^{Thr}$ was likely to cause a decrease in the efficiency and/or fidelity of mitochondrial protein synthesis, which could explain the clinical symptoms of patients carrying the G30A mutation in $hmtRNA^{Thr}$, namely hearing loss, muscle weakness, and focal COX deficiency (17). Interestingly, A38 also functions as a critical nucleotide determinant in the t^6A modification, at least for $hmtRNA^{Thr}$. The t^6A modification contributes to the formation of canonical U-turn structure of the anticodon loop by preventing U33–A37 base pairing, which suggested that the A38G mutation in $hmtRNA^{Thr}$ probably affected the structure of the anticodon loop (40). In addition, C32 and A38 tend to form a non-Watson–Crick pair during decoding (43). The A38G mutation would make the C32 and G38 form a strong Watson–Crick pair, which might also affect the structure of the anticodon loop, consistent with the increased T_m value of the A38G mutant. U36 and A37 bases have been suggested to be the identity determinants in t^6A formation in *Xenopus laevis* oocyte cytoplasm (51). Despite A38 being a critical element in t^6A formation in $hmtRNA^{Thr}$ and tRNAs in *Xenopus laevis* oocyte cytoplasm (51), G38 is found in human and bovine mitochondrial t^6A37-contained $tRNA^{Ile}$s (4,39). Therefore, the systematic study of identity determinants of t^6A37 formation in mitochondria should be further explored. The deficiency in aminoacylation and t^6A modification of the A38G mutant implied low translational fidelity and efficiency in mitochondria, which might contribute to the symptoms of complex III and IV deficiency in tissues and sudden multisystem failure (18).

In summary, we propose a model of the potential molecular pathogenesis of the G30A and A38G mutations, which alter the anticodon stem and/or loop structure of $hmtRNA^{Thr}$. The two mutations result in decreased aminoacylation, editing, and t^6A modification, which likely lead to low accuracy and efficiency of mitochondrial protein synthesis (Figure 9).

SUPPLEMENTARY DATA

Supplementary Data are available at NAR Online.

ACKNOWLEDGEMENTS

We are grateful to Dr Qing-Fei Yin and Prof. Fei-Long Meng (Shanghai Institute of Biochemistry and Cell Biology), and Dr Meng Wang (Zhejiang University) for their valuable suggestions in tRNA structure probing assay, and Prof. Söll Dieter (Yale University) for reading the manuscript.

FUNDING

National Key Research and Development Program of China [2017YFA0504000]; National Natural Science Foundation of China [31670801, 91440204, 31570792]; Strategic Priority Research Program of the Chinese Academy of Sciences [XDB19000000]; Shanghai Rising-Star Program [16QA1404400]; Youth Innovation Promotion Association (Chinese Academy of Sciences) [Y119S41291 to X.-L.Z.]. Funding for open access charge: The National Key Research and Development Program of China [2017YFA0504000].
Conflict of interest statement. None declared.

REFERENCES

1. Wallace,D.C. (2005) A mitochondrial paradigm of metabolic and degenerative diseases, aging, and cancer: a dawn for evolutionary medicine. *Annu. Rev. Genet.*, **39**, 359–407.
2. Anderson,S., Bankier,A.T., Barrell,B.G., de Bruijn,M.H., Coulson,A.R., Drouin,J., Eperon,I.C., Nierlich,D.P., Roe,B.A., Sanger,F. *et al.* (1981) Sequence and organization of the human mitochondrial genome. *Nature*, **290**, 457–465.
3. Dudek,J., Rehling,P. and van der Laan,M. (2013) Mitochondrial protein import: common principles and physiological networks. *Biochim. Biophys. Acta*, **1833**, 274–285.
4. Suzuki,T., Nagao,A. and Suzuki,T. (2011) Human mitochondrial tRNAs: biogenesis, function, structural aspects, and diseases. *Annu. Rev. Genet.*, **45**, 299–329.
5. Suzuki,T., Nagao,A. and Suzuki,T. (2011) Human mitochondrial diseases caused by lack of taurine modification in mitochondrial tRNAs. *Wiley Interdiscip. Rev. RNA*, **2**, 376–386.
6. Levinger,L., Morl,M. and Florentz,C. (2004) Mitochondrial tRNA 3′ end metabolism and human disease. *Nucleic Acids Res.*, **32**, 5430–5441.
7. Hao,R., Yao,Y.N., Zheng,Y.G., Xu,M.G. and Wang,E.D. (2004) Reduction of mitochondrial tRNALeu(UUR) aminoacylation by some MELAS-associated mutations. *FEBS Lett.*, **578**, 135–139.
8. Hao,R., Zhao,M.W., Hao,Z.X., Yao,Y.N. and Wang,E.D. (2005) A T-stem slip in human mitochondrial tRNALeu(CUN) governs its charging capacity. *Nucleic Acids Res.*, **33**, 3606–3613.
9. Shoffner,J.M., Lott,M.T., Lezza,A.M., Seibel,P., Ballinger,S.W. and Wallace,D.C. (1990) Myoclonic epilepsy and ragged-red fiber disease (MERRF) is associated with a mitochondrial DNA tRNA(Lys) mutation. *Cell*, **61**, 931–937.
10. Yasukawa,T., Suzuki,T., Ishii,N., Ohta,S. and Watanabe,K. (2001) Wobble modification defect in tRNA disturbs codon-anticodon interaction in a mitochondrial disease. *EMBO J.*, **20**, 4794–4802.
11. Wang,M., Zhou,X.L., Liu,R.J., Fang,Z.P., Zhou,M., Eriani,G. and Wang,E.D. (2013) Multilevel functional and structural defects induced by two pathogenic mitochondrial tRNA mutations. *Biochem. J.*, **453**, 455–465.
12. Ibba,M. and Soll,D. (1999) Quality control mechanisms during translation. *Science*, **286**, 1893–1897.
13. Tan,M., Zhu,B., Zhou,X.L., He,R., Chen,X., Eriani,G. and Wang,E.D. (2010) tRNA-dependent pre-transfer editing by prokaryotic leucyl-tRNA synthetase. *J. Biol. Chem.*, **285**, 3235–3244.
14. Sankaranarayanan,R., Dock-Bregeon,A.C., Romby,P., Caillet,J., Springer,M., Rees,B., Ehresmann,C., Ehresmann,B. and Moras,D. (1999) The structure of threonyl-tRNA synthetase-tRNA(Thr) complex enlightens its repressor activity and reveals an essential zinc ion in the active site. *Cell*, **97**, 371–381.
15. Lee,J.W., Beebe,K., Nangle,L.A., Jang,J., Longo-Guess,C.M., Cook,S.A., Davisson,M.T., Sundberg,J.P., Schimmel,P. and Ackerman,S.L. (2006) Editing-defective tRNA synthetase causes protein misfolding and neurodegeneration. *Nature*, **443**, 50–55.
16. Hilander,T., Zhou,X.L., Konovalova,S., Zhang,F.P., Euro,L., Chilov,D., Poutanen,M., Chihade,J., Wang,E.D. and Tyynismaa,H. (2018) Editing activity for eliminating mischarged tRNAs is essential in mammalian mitochondria. *Nucleic Acids Res.*, **46**, 849–860.
17. Nishino,I., Seki,A., Maegaki,Y., Takeshita,K., Horai,S., Nonaka,I. and Goto,Y. (1996) A novel mutation in the mitochondrial tRNA(Thr) gene associated with a mitochondrial encephalomyopathy. *Biochem. Biophys. Res. Commun.*, **225**, 180–185.
18. Yoon,K.L., Ernst,S.G., Rasmussen,C., Dooling,E.C. and Aprille,J.R. (1993) Mitochondrial disorder associated with newborn cardiopulmonary arrest. *Pediatr. Res.*, **33**, 433–440.

19. Yoon,K.L., Aprille,J.R. and Ernst,S.G. (1991) Mitochondrial tRNA(thr) mutation in fatal infantile respiratory enzyme deficiency. *Biochem. Biophys. Res. Commun.*, **176**, 1112–1115.
20. Seneca,S., Lissens,W., Liebaers,I., van den Bergh,P., Nassogne,M.C., Benatar,A. and de Meirleir,L. (1998) Pitfalls in the diagnosis of mtDNA mutations. *J. Med. Genet.*, **35**, 963–964.
21. Grasbon-Frodl,E.M., Kosel,S., Sprinzl,M., von Eitzen,U., Mehraein,P. and Graeber,M.B. (1999) Two novel point mutations of mitochondrial tRNA genes in histologically confirmed Parkinson disease. *Neurogenetics*, **2**, 121–127.
22. Li,R., Qu,J., Zhou,X., Tong,Y., Hu,Y., Qian,Y., Lu,F., Mo,J.Q., West,C.E. and Guan,M.X. (2006) The mitochondrial tRNA(Thr) A15951G mutation may influence the phenotypic expression of the LHON-associated ND4 G11778A mutation in a Chinese family. *Gene*, **376**, 79–86.
23. Salinas-Giege,T., Giege,R. and Giege,P. (2015) tRNA biology in mitochondria. *Int. J. Mol. Sci.*, **16**, 4518–4559.
24. Murphy,F.V.T., Ramakrishnan,V., Malkiewicz,A. and Agris,P.F. (2004) The role of modifications in codon discrimination by tRNA(Lys)UUU. *Nat. Struct. Mol. Biol.*, **11**, 1186–1191.
25. Weissenbach,J. and Grosjean,H. (1981) Effect of threonylcarbamoyl modification (t6A) in yeast tRNA Arg III on codon-anticodon and anticodon-anticodon interactions. A thermodynamic and kinetic evaluation. *Eur. J. Biochem.*, **116**, 207–213.
26. Lin,C.A., Ellis,S.R. and True,H.L. (2010) The Sua5 protein is essential for normal translational regulation in yeast. *Mol. Cell. Biol.*, **30**, 354–363.
27. Wan,L.C.K., Mao,D.Y.L., Neculai,D., Strecker,J., Chiovitti,D., Kurinov,I., Poda,G., Thevakumaran,N., Yuan,F., Szilard,R.K. *et al.* (2013) Reconstitution and characterization of eukaryotic N6-threonylcarbamoylation of tRNA using a minimal enzyme system. *Nucleic Acids Res.*, **41**, 6332–6346.
28. Lauhon,C.T. (2012) Mechanism of N6-threonylcarbamoyladenonsine (t(6)A) biosynthesis: isolation and characterization of the intermediate threonylcarbamoyl-AMP. *Biochemistry*, **51**, 8950–8963.
29. Wang,Y., Zhou,X.L., Ruan,Z.R., Liu,R.J., Eriani,G. and Wang,E.D. (2016) A human disease-causing point mutation in mitochondrial threonyl-tRNA synthetase induces both structural and functional defects. *J. Biol. Chem.*, **291**, 6507–6520.
30. Fechter,P., Rudinger,J., Giege,R. and Theobald-Dietrich,A. (1998) Ribozyme processed tRNA transcripts with unfriendly internal promoter for T7 RNA polymerase: production and activity. *FEBS Lett.*, **436**, 99–103.
31. Zhou,X.L., Du,D.H., Tan,M., Lei,H.Y., Ruan,L.L., Eriani,G. and Wang,E.D. (2011) Role of tRNA amino acid-accepting end in aminoacylation and its quality control. *Nucleic Acids Res.*, **39**, 8857–8868.
32. Jorgensen,R., Sogaard,T.M., Rossing,A.B., Martensen,P.M. and Justesen,J. (2000) Identification and characterization of human mitochondrial tryptophanyl-tRNA synthetase. *J. Biol. Chem.*, **275**, 16820–16826.
33. Zhou,X.L., Ruan,Z.R., Huang,Q., Tan,M. and Wang,E.D. (2013) Translational fidelity maintenance preventing Ser mis-incorporation at Thr codon in protein from eukaryote. *Nucleic Acids Res.*, **41**, 302–314.
34. Arnion,H., Korkut,D.N., Masachis Gelo,S., Chabas,S., Reignier,J., Iost,I. and Darfeuille,F. (2017) Mechanistic insights into type I toxin antitoxin systems in Helicobacter pylori: the importance of mRNA folding in controlling toxin expression. *Nucleic Acids Res.*, **45**, 4782–4795.
35. Lundin,K., Wilichowski,E., Ernst,B.P. and Hanefeld,F. (1997) S1 nuclease hybrid analysis of mitochondrial DNA amplified by long-distance PCR: rapid screening for small-scale rearrangements. *Nucleic Acids Res.*, **25**, 2535–2536.
36. Shenk,T.E., Rhodes,C., Rigby,P.W. and Berg,P. (1975) Biochemical method for mapping mutational alterations in DNA with S1 nuclease: the location of deletions and temperature-sensitive mutations in simian virus 40. *Proc. Natl. Acad. Sci. U.S.A.*, **72**, 989–993.
37. Silvestri,G., Mongini,T., Odoardi,F., Modoni,A., deRosa,G., Doriguzzi,C., Palmucci,L., Tonali,P. and Servidei,S. (2000) A new mtDNA mutation associated with a progressive encephalopathy and cytochrome c oxidase deficiency. *Neurology*, **54**, 1693–1696.
38. Kirino,Y., Yasukawa,T., Ohta,S., Akira,S., Ishihara,K., Watanabe,K. and Suzuki,T. (2004) Codon-specific translational defect caused by a wobble modification deficiency in mutant tRNA from a human mitochondrial disease. *Proc. Natl. Acad. Sci. U.S.A.*, **101**, 15070–15075.
39. Suzuki,T. and Suzuki,T. (2014) A complete landscape of post-transcriptional modifications in mammalian mitochondrial tRNAs. *Nucleic Acids Res.*, **42**, 7346–7357.
40. Stuart,J.W., Gdaniec,Z., Guenther,R., Marszalek,M., Sochacka,E., Malkiewicz,A. and Agris,P.F. (2000) Functional anticodon architecture of human tRNALys3 includes disruption of intraloop hydrogen bonding by the naturally occurring amino acid modification, t6A. *Biochemistry*, **39**, 13396–13404.
41. Hedges,S.B., Dudley,J. and Kumar,S. (2006) TimeTree: a public knowledge-base of divergence times among organisms. *Bioinformatics*, **22**, 2971–2972.
42. Zhou,X.L., Ruan,Z.R., Wang,M., Fang,Z.P., Wang,Y., Chen,Y., Liu,R.J., Eriani,G. and Wang,E.D. (2014) A minimalist mitochondrial threonyl-tRNA synthetase exhibits tRNA-isoacceptor specificity during proofreading. *Nucleic Acids Res.*, **42**, 13873–13886.
43. Grosjean,H. and Westhof,E. (2016) An integrated, structure- and energy-based view of the genetic code. *Nucleic Acids Res.*, **44**, 8020–8040.
44. Holman,K.M., Wu,J., Ling,J. and Simonovic,M. (2016) The crystal structure of yeast mitochondrial ThrRS in complex with the canonical threonine tRNA. *N Nucleic Acids Res.*, **44**, 1428–1439.
45. Hasegawa,T., Miyano,M., Himeno,H., Sano,Y., Kimura,K. and Shimizu,M. (1992) Identity determinants of E. coli threonine tRNA. *Biochem. Biophys. Res. Commun.*, **184**, 478–484.
46. Nameki,N. (1995) Identity elements of tRNA(Thr) towards Saccharomyces cerevisiae threonyl-tRNA synthetase. *Nucleic Acids Res.*, **23**, 2831–2836.
47. Nameki,N., Asahara,H. and Hasegawa,T. (1996) Identity elements of Thermus thermophilus tRNA(Thr). *FEBS Lett.*, **396**, 201–207.
48. Schulman,L.H. and Pelka,H. (1990) An anticodon change switches the identity of E. coli tRNA(mMet) from methionine to threonine. *Nucleic Acids Res.*, **18**, 285–289.
49. Giege,R., Sissler,M. and Florentz,C. (1998) Universal rules and idiosyncratic features in tRNA identity. *Nucleic Acids Res.*, **26**, 5017–5035.
50. Hampsey,M., Na,J.G., Pinto,I., Ware,D.E. and Berroteran,R.W. (1991) Extragenic suppressors of a translation initiation defect in the cyc1 gene of Saccharomyces cerevisiae. *Biochimie*, **73**, 1445–1455.
51. Morin,A., Auxilien,S., Senger,B., Tewari,R. and Grosjean,H. (1998) Structural requirements for enzymatic formation of threonylcarbamoyladenosine (t6A) in tRNA: an in vivo study with Xenopus laevis oocytes. *RNA*, **4**, 24–37.